Oscillations of aqueous PEDOT:PSS fluid droplets and the properties of complex fluids in drop-on-demand inkjet printing

CrossMark

Stephen D. Hoath [a,*], Wen-Kai Hsiao [a,1], Graham D. Martin [a], Sungjune Jung [b], Simon A. Butler [c], Neil F. Morrison [d], Oliver G. Harlen [d], Lisong S. Yang [e], Colin D. Bain [e], Ian M. Hutchings [a]

[a] University of Cambridge, Department of Engineering, Cambridge CB3 0FS, UK
[b] Pohang University of Science and Technology, Department of Creative IT Engineering, South Korea
[c] University of Cambridge, Department of Chemical Engineering and Biotechnology, Cambridge CB2 3RA, UK
[d] University of Leeds, School of Mathematics, Leeds LS2 9JT, UK
[e] University of Durham, Department of Chemistry, Durham DH1 3LE, UK

ABSTRACT

Shear-thinning aqueous poly(3,4-ethylenedioxythiophene): poly(styrene sulphonate) (PEDOT:PSS) fluids were studied under the conditions of drop-on-demand inkjet printing. Ligament retraction caused oscillation of the resulting drops, from which values of surface tension and viscosity were derived. Effective viscosities of <4 mPa s at drop oscillation frequencies of 13–33 kHz were consistent with conventional high-frequency rheometry, with only a small possible contribution from viscoelasticity with a relaxation time of about 6 μs. Strong evidence was found that the viscosity, reduced by shear-thinning in the print-head nozzle, recovered as the drop formed. The low viscosity values measured for the drops in flight were associated with the strong oscillation induced by ligament retraction, while for a weakly perturbed drop the viscosity remained high. Surface tension values in the presence of surfactant were significantly higher than the equilibrium values, and consistent with the surface age of the drops.
© 2015 The Authors. Published by Elsevier B.V. This is an open access article under the CC BY license (http://creativecommons.org/licenses/by/4.0/).

1. Introduction

Inkjet printing commonly involves the use of fluids with complex rheology [1], primarily to achieve the required properties on the substrate but also to achieve reliable jet and drop formation. Aqueous PEDOT:PSS (poly(3,4-ethylenedioxythiophene): poly(-styrene sulphonate)) is an example of such a fluid, commonly printed to form transparent conductors [2,3]. It has been shown to behave particularly well in drop-on-demand (DoD) inkjet printing [4] in comparison with Newtonian fluids exposed to the same conditions. [5] Typical shear rates are $>10^5 \, s^{-1}$ within the small nozzles (with diameter ca. 40 μm) employed in DoD printing, for jet velocities of the order of 5 m s^{-1}, well beyond the range of measurement of conventional rheometers. Once outside the nozzle, conditions within the fluid jet involve much lower shear rates, with

two major exceptions. The first occurs locally at points where the jet necks down as it pinches off. The second occurs if the drop oscillates in shape. Data from the work of Brenn and Teichtmeister [6] can be used to estimate that very high shear rates ($>10^5 \, s^{-1}$) will occur within oscillating drops with sizes typical of DoD printing (i.e. with diameters of the order of 50 μm).

High frequency rheological measurements show aqueous PEDOT:PSS to be highly shear-thinning. It also has a marked tendency to form fewer satellite drops (by break-up of the jet behind the main drop) in DoD printing than Newtonian fluids under the same printing conditions [4]. Reduction or elimination of satellite drop production is of key importance in inkjet printing for functional applications.

Although the recovery time for many shear-thinning fluids can be >1 s, recent studies [7] have suggested that the delays observed in ligament break-up for aqueous PEDOT:PSS solutions are consistent with much shorter times (≪100 μs) for the recovery of high viscosity once the jet is outside the nozzle, following the high shear-rate conditions (and resulting low viscosity) within the nozzle. However, interpretation of the data is possibly complicated by the presence of viscoelasticity, and also by the uncertain influence of the surfactant added to PEDOT:PSS formulations for practical

---

* Corresponding author. Tel.: +44 1223 764626; fax: +44 1223 464217.
  E-mail address: sdh35@cam.ac.uk (S.D. Hoath).
[1] Current address: Research Center Pharmaceutical Engineering (RCPE) GmbH, Graz, Austria.

printing applications. The present work uses measurements of the oscillation of drops generated from a DoD print-head to explore shear thinning and recovery, viscoelasticity and time-dependent surface tension in drops of the appropriate size for inkjet printing.

Oscillation of a printed drop in free flight may be initiated by the retraction of an attached ligament or by coalescence with a second drop either leading or trailing the main drop. Dynamic measurements of viscosity and surface tension can be extracted from the decay rates and frequencies of the resulting oscillation. [8–10] Lamb [11] showed that for Newtonian fluids, where the restoring force is due to the surface tension and the damping is provided by viscosity, for small amplitudes the fundamental free shape ($l = 2$) mode of oscillation will dominate. A non-Newtonian fluid will respond like a Newtonian fluid with a viscosity appropriate to the drop oscillation frequency. This dynamic viscosity determines the decay rate of the oscillations. The surface tension may be altered by the diffusion of surfactants to the newly created fluid surface; the oscillating drop provides information relevant to the surface age of a printed drop in flight, which will typically be smaller by a factor of 10^2-10^3 than the >0.01 s timescale over which dynamic surface tension is conventionally measured [4,10].

Drop oscillation will also be affected by viscoelastic behaviour in the fluid [12] and it is possible that this might be more important than shear-thinning in its effect on the production of satellite drops [4], although simulations of DoD jetting behaviour using the Carreau model for shear-thinning [13] have suggested that satellite suppression is possible without invoking viscoelastic behaviour. The use of a Giesekus model [14,15] might allow the incorporation of elasticity, but under DoD printing conditions it predicts only moderate (<2-fold) shear-thinning, far less than that observed in aqueous PEDOT:PSS. The theory for viscoelastic drop oscillations by Khismatullin and Nadim [12] has been recently extended by Brenn and Teichtmeister [6]. These papers show a small influence of elasticity on the oscillation frequency of viscoelastic drops and indicate how measurements of rheological behaviour and oscillation decay rate might be used to estimate upper limits for a viscoelastic relaxation time.

2. Models for drop oscillation

Rayleigh [16] investigated the free axisymmetric oscillation of an inviscid drop in the small amplitude, linear regime. He described the distortion of the spherical drop by an infinite series of orthogonal surface spherical harmonics, i.e. natural oscillation modes. The axisymmetric form is:

$$r(\theta, t) = r_0 \left[1 + \sum_{l=2}^{\infty} a_l(t) P_l(\cos \theta) \right] \tag{1}$$

where $P_l(\cos \theta)$ are the Legendre polynomials, r_0 is the unperturbed radius of the drop, a_l is the amplitude of the lth mode of oscillation (with fundamental mode $l = 2$), and θ is the polar angle of the spherical coordinate system with its origin at the centre of the drop. The angular frequency Ω_l of the lth oscillation mode is given by

$$\Omega_l = \sqrt{\sigma \frac{l(l-1)(l+2)}{\rho r_0^3}}, \tag{2}$$

where σ and ρ are the surface tension and density of the fluid, respectively.

For viscous liquids and an oscillation amplitude that is small compared to r_0, Lamb [11] obtained an irrotational approximation. If the oscillation amplitude decays exponentially as $A_l \exp(-t/\tau_l)$, then the decay time τ_l and the angular frequency of oscillation Ω_l^* are given by

$$\tau_l = \frac{\rho r_0^2}{\eta(l-1)(2l+1)} \tag{3}$$

and

$$\Omega_l^* = \Omega_l \sqrt{1 - (\Omega_l \tau_l)^{-2}} \tag{4}$$

where η is the viscosity of the fluid. Prosperetti [17] and Becker et al. [18] pointed out that for Ohnesorge number $Oh = \eta/(\rho \sigma r_0)^{1/2}$ < 0.1 and small oscillations of fundamental mode $l = 2$ with amplitude not exceeding 0.1 r_0, Eqs. (3) and (4) will apply. Even for initial amplitudes as large as 0.2 r_0, the change in fundamental frequency Ω_2 (i.e. Ω_l where $l = 2$) is 2.5%. [18] Smith [19] has shown that the time-dependent variations in the decay factor of the fundamental mode for oscillation amplitudes as large as 0.3 r_0 can be approximated by an additional component that is quadratic in this amplitude and less than 25% below the linear result, even at this limit.

Computer simulations for generalised Newtonian fluids suggest that the shear rate within a jetted ligament falls rapidly after it leaves the nozzle, with the major contributions to high shear-rate arising from the velocity variation in the outer surface of the ligament. The outermost regions of drops are significant for vorticity in shape oscillations. [17]

Eq. (4) implies that the shape will not oscillate but the deformation will decay aperiodically if $\Omega_l < 1/\tau_l$; for example, for drops of 50 μm diameter with the density of water and a surface tension of 32 mN/m, the viscosity must be less than 16 mPa s for oscillation to occur.

Linear viscoelastic behaviour in a polymer solution can be modelled by a (viscous) dashpot in series with a parallel combination of a linear (elastic) spring and another (viscous) dashpot, yielding [12] the Jeffreys constitutive equation relating the deviatoric stress τ and rate of strain $\dot{\gamma}$:

$$\tau + \lambda_1 \frac{\partial \tau}{\partial t} = 2\eta \left(\dot{\gamma} + \lambda_2 \frac{\partial \dot{\gamma}}{\partial t} \right) \tag{5}$$

λ_1 and λ_2 represent the relaxation and retardation times respectively, where $0 \leqslant \lambda_2 \leqslant \lambda_1$. If $\lambda_1 = \lambda_2$ the response is Newtonian while $\lambda_2 = 0$ corresponds to the Maxwell model of a simple series combination of a dashpot and spring. The ratio of solvent and solution viscosities is λ_2/λ_1. Relaxation and retardation Deborah numbers De_1 and De_2 are defined by $De_1 = \lambda_1 \Omega_2$ and $De_2 = \lambda_2 \Omega_2$. The ratio between the viscosities for the solvent and the solution is De_2/De_1. Khismatullin and Nadim [12] consider asymptotic limits that are useful here. In the limit of low Deborah number, the drop oscillation frequency is Ω_2^* given by Eq. (4). Aqueous PEDOT:PSS fluid droplets with a high shear rate viscosity of 3 mPa s have a sufficiently high Reynolds number ($Re = 26$) that drop oscillation theory pertinent to low viscosity conditions should apply. For aqueous 1.1 wt% PEDOT:PSS fluid drops with a viscosity of 75 mPa s (which should prevent oscillation) Re would be reduced to order unity. Calculations were made using the full theory [12] rather than with $De_2 = 0$ asymptotic limits to explore both periodic damped oscillations and aperiodic (over-damped) conditions. The results are discussed more fully below, but it is useful to explore the asymptotic solutions here.

At high fluid viscosities where the system is over-damped, the distortion decays exponentially with both a slow rate arising from surface tension, and a fast decay rate driven by the viscosity only [12]. The slow exponential decay rate δ_1 is given by

$$\delta_1 = \frac{l(l+2)(2l+1)\sigma}{2(2l^2+4l+3)\eta R} = \frac{20}{19} \frac{\sigma}{\eta R} \quad \text{for the } l = 2 \text{ mode.} \tag{6}$$

The fast decay rate δ_2 is given by:

$$\delta_2 = \frac{2(l-1)(2l^2 + 4l + 3)\eta}{(2l+1)(1+E_l)\rho R^2} \cong 6.90\,\frac{\eta}{\rho R^2} \quad \text{for the } l = 2 \text{ mode.}$$

(7)

The mode-dependent term [12] $E_l = 4l(l-1)(l+2)/[(2l+1)(2l+3)(2l+5)]$ is always small ($\leqslant 1/2$). For the fluid properties and drop sizes considered in this work, $1/\delta_1 \approx 30\,\mu s$ and $1/\delta_2 \ll 1\,\mu s$, so that the slow decay process dominates for all practical purposes. Measurement of aperiodic shape decay (for a drop of known size) can therefore provide a measurement of the ratio σ/η.

In the low viscosity limit, for oscillating drops, the viscoelastic correction to Eq. (3) involves replacing viscosity η by $\eta'(\Omega_2)$, the real part of the complex viscosity at frequency Ω_2, where $\eta' = \eta(1 + De_1 De_2)/(1 + De_1^2)$, since the decay rate is determined by the component of the stress in phase with the velocity, according to Khismatullin and Nadim [12]. To leading order the frequency of drop oscillation Ω is given by:

$$\Omega^2 = \Omega_2^2 + 5\eta''/(\rho R^2)$$

(8)

where $\eta'' = \eta(De_1 - De_2)/(1 + De_1^2)$ is the out-of-phase component of the complex viscosity and represents the additional "spring-stiffness" that is provided by the elastic stress component acting in synchronism with the surface tension. For small De_2/De_1, the maximum oscillation frequency for viscoelastic drops corresponds to $De_1 \approx 1$ in the asymptotic limit. For such rapidly recovering weakly viscoelastic fluid drops, the predicted asymptotic effects on frequency are small. For $De_2 = De_1$, the solvent and the solution have the same viscosity and are dynamically equivalent, and so there is no effect of elasticity on the oscillation frequency or decay.

3. Experimental methods and materials

3.1. Drop formation and imaging

A single-nozzle piezoelectric print-head with diamond-like carbon coating and a 40 μm diameter nozzle (MJ-ABP, MicroFab Technologies Inc., TX, USA) was used to generate oscillating fluid drops 30 to 60 μm in diameter. A high-speed video camera (Shimadzu HPV-1) recorded enlarged images of the drops via a × 10 Mitutoyo objective lens (NA = 0.28) and Navitar × 12 telescopic system. The camera recorded a maximum of 102 frames at an exposure time of 0.5 μs at rates of either 5×10^5 or 10^6 frames per second (fps), with the image sensor internally cooled to 10 °C, at various exposure and low gain settings. The imaging delay time was adjusted until drop oscillation sequences could be properly captured. Image files were analysed with IrfanView, Visual Basic and MatLab software. The image magnification was calibrated by imaging long wires of 104 μm diameter and the uncertainty in drop diameter resulting from pixelation and edge detection was ±1 μm.

Fig. 1 shows the typical evolution of jetted material. The first frame shows a drop with a substantial tapering ligament extending from the nozzle just visible at the top of the image. As time progresses the ligament retracts into the drop, which is markedly distorted and then oscillates towards its final, near-spherical shape as it travels downwards. Images which were measured to generate the data reported below were captured at later times when the deformation was more symmetrical and was dominated by the fundamental $l = 2$ mode.

3.2. Fluids

Aqueous solutions of PEDOT:PSS, as listed in Table 1, were prepared by diluting a commercial solution (Heraeus Clevios PH 1000,
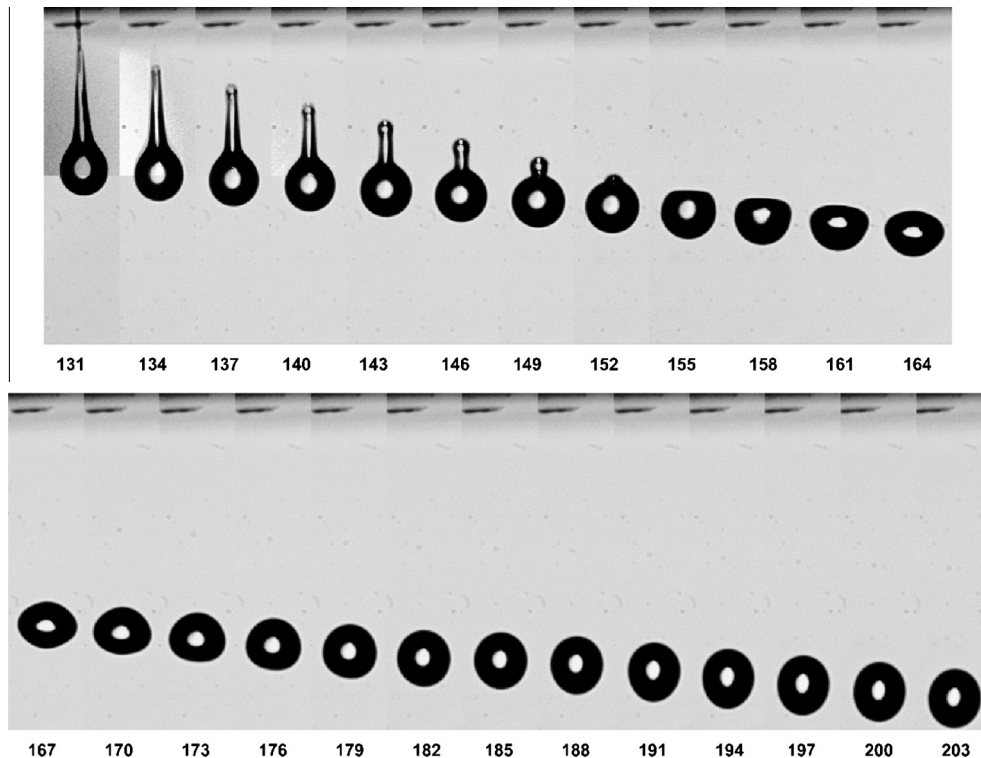
Fig. 1. Images taken from a sequence captured at 10^6 frames per second showing drop formation and subsequent oscillation. The liquid was aqueous 1.1 wt% PEDOT:PSS with 0.33 wt% Dynol 607. Times (in microseconds) are shown after jet tip emergence from the 40 μm diameter nozzle exit (visible at the top of each frame).

Table 1
Physical properties for pure water (top line) and various concentrations of PEDOT:PSS in water with and without the addition of Dynol 607 (D) and Zonyl FSO-100 (Z) surfactants or isopropanol (IPA). Concentrations are given in wt%. Densities are taken from standard data tables. [20] Entries marked ¶ are estimated values.
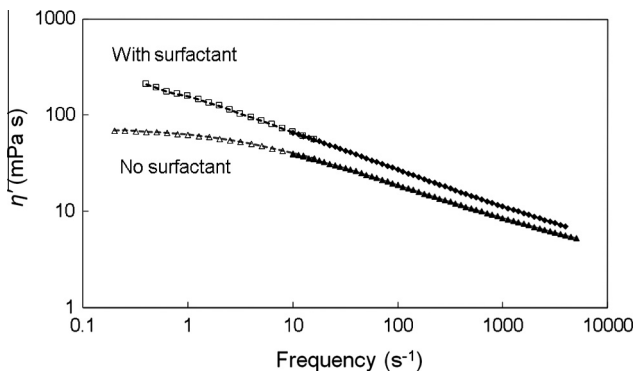
PEDOT:PSS (wt%)	Surfactant	η' (mPa s) at 1 s^{-1}	η' (mPa s) at 4000 s^{-1}	σ (mN/m)	ρ (kg/m^3)
0	None	1.0	1.0	72.8	1000
1.1	None	63	6.3	70 ± 3	1000
0.8	None	26	4.1	70 ± 3	1000
1.1	0.23% D + 0.27% Z	156	8.2	21 ± 2	1000
0.8	0.23% D + 0.27% Z	41	4.2	21 ± 2	1000
0.8	0.06% D	25	4¶	30±1	1000
0.8	30% IPA	25	4¶	30±1	780
1.1	0.33% D	68	9¶	30¶	1000
1.1	0.66% D	68	9¶	30¶	1000

1.1 wt% solids in water, 1:2.5 PEDOT:PSS by weight, gel particle size d_{50} = 25 nm) with deionised water. One set contained 1.1 wt% and 0.8 wt% solids, with and without the addition of two low molecular weight (<1 kDa) surfactants: 0.23 wt% Dynol 607 and 0.27 wt% Zonyl FSO-100. These formulations were chosen as representative of those used for printed electronics. Other fluids used to further explore the effects of surfactants contained 0.8 wt% PEDOT:PSS with either 0.06 wt% Dynol 607 surfactant or 30 wt% isopropanol (IPA). Dynol 607 has a maximum solubility in water of 0.032 wt% and the excess surfactant additive will therefore tend to stabilise the PEDOT:PSS particles [8].

Equilibrium surface tension was measured at 21 °C with a SITA pro line t-15 bubble tensiometer. Rheological measurements were performed with an ARES rheometer at shear rates up to 15 s^{-1} and with a piezo axial vibrator [21] (PAV) at frequencies up to 6 kHz. Table 1 shows the measured values of viscosity (the real component η' of complex viscosity) at 1 s^{-1} and 4000 s^{-1} and of surface tension for the solutions with and without the surfactant mixture. For the most concentrated (1.1 wt%) solution, viscosity fell from >60 mPa s at low shear rate to about 4 mPa s at the highest shear rates. The PEDOT:PSS fluids also exhibited elasticity that steadily reduced with increasing frequency [4]. All the aqueous PEDOT:PSS solutions shear-thinned significantly, but the presence of surfactants did not affect the trends in the rheological behaviour, particularly at the higher frequencies (10–4000 s^{-1}).

Fig. 2 shows the viscous component η' defined by $G''/(2\pi f)$ for 1.1 wt% PEDOT:PSS with and without a total of 0.5 wt% surfactant, measured at frequencies from 0.4 to 4000 s^{-1} by ARES (open symbols) and PAV (solid symbols). The ARES values were higher than the PAV data due to solvent evaporation, and have been normalised to the PAV values at the overlapping frequency range of about 10 s^{-1}.

The surfactant additives increased the viscosity for all the PEDOT:PSS suspensions especially at lower frequencies (<10 s^{-1}),

with significant non-linear dependence on the concentration of PEDOT:PSS. At the highest frequency (4 kHz), the viscosities of the 1.1 wt% PEDOT:PSS solutions with and without surfactant approached similar values, to within 30%. Even at a frequency of 1 s^{-1} the values of η' with and without the surfactant additives lay within a factor of two, and therefore the effect of adding 0.5 wt% D + Z surfactants on viscosity appears small. The elastic component η'' of complex viscosity was always smaller than η' at all frequencies. The frequency variations of viscosity were fitted with Carreau and power law models for later comparison with the viscosity values deduced from the oscillating drops.

3.3. Image analysis and data extraction

For the oscillation of drops generated in drop-on-demand printing the effect of gravity is negligible, all the oscillation modes are exponentially damped, and damping is so much faster for the higher modes that the behaviour at longer times is dominated by the $l = 2$ mode. For these slowly moving drops, aerodynamic effects on the drop shape are expected to be small. Therefore if the fluid density is known, the surface tension and viscosity can be extracted by fitting the observed behaviour to that predicted for the $l = 2$ mode. Surfactant diffusion rates, drop size, ligament collapse into the drop and surface age may all influence the effective value of dynamic surface tension for complex fluids containing surfactants.

We measured up-down (along the jet axis, in our experiments, vertical) and left–right (i.e. horizontal) dimensions of the drop images: i.e. the polar and equatorial diameters. For small amplitudes such measurements are sensitive only to the even order modes of oscillation, but odd orders of drop shape may also appear initially when there is a large axial impulse such as that caused by the ligament impact shown in Fig. 1.

For the $l = 2$ mode, Eq. (1) reduces to:

$$r(\theta, t) = r_0\left[1 + \frac{1}{2}a_2(t)(3\cos^2\theta - 1)\right]. \tag{9}$$

The polar diameter of the drop $L = 2r_0[1 + a_2(t)]$ and equatorial diameter $W = r_0[2 - a_2(t)]$. The amplitude $a_2(t)$ of the fundamental $l = 2$ mode is calculated from $r_0 a_2(t) = (L - W)/3$.

The measured time-dependent oscillation amplitude is fitted to the functional form

$$a_2(t) = A \cdot \exp\left(-\frac{t}{\tau}\right)\cos\left(\frac{2\pi t}{T}\right) + a_{offset} \tag{10}$$

where A is the oscillation amplitude at time $t = 0$ relative to a time offset t_0, τ is the decay time and T is the oscillation period from which $\Omega = 2\pi/T$. As the initial data may be distorted by the effects of the impinging ligament, these points were excluded from the fit. The maximum instantaneous amplitude at the start of the fitted period was usually less than 3 μm (i.e. <20% of the drop radius).

Fig. 2. The viscous component η' of complex viscosity η^* for aqueous 1.1 wt% PEDOT:PSS with and without 0.23 wt% Dynol 607 and 0.27 wt% Zonyl FSO-100 surfactants, measured by ARES (open symbols) and PAV (solid symbols), normalised to coincide at the overlap frequency of 10 s^{-1}.

Finite values of the asymmetry a_{offset} can be interpreted as an indicator of large amplitude changes.
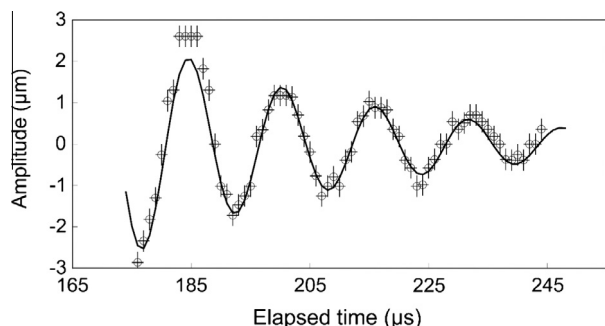
The fluid viscosity is calculated from Eq. (3) and the effective surface tension from Eqs. (2) and (4). The drop dimensions were determined from the images to an accuracy of 1 μm, or about 2% of the diameter. The dominant errors in the data extracted from the images were in the vertical and horizontal dimensions of the drops, rather than in the times, as indicated by the error bars in the resulting graphs. The uncertainties in the derived values of surface tension and viscosity were estimated for representative drops by analysing sets of data with the extreme values represented by the measurement errors. This suggested confidence limits for surface tension and viscosity of ±10% and ±20% respectively.

4. Results

A test of the capability of the experimental method is provided by the use of pure (deionized) water. Fig. 3 shows the data recorded for a 31 μm diameter drop ejected from the print-head, plotted in terms of the amplitude $(L-W)/3$, together with the behaviour predicted by Eqs. (9) and (10) based on a least-squares fit to the data. The curve has an initial amplitude $r_0 a_2$ of 1.5 μm (i.e. 10% of the drop radius) and a frequency of 63 kHz, and takes account of only the $l = 2$ mode; it includes a small zero offset (<0.1 μm). The liquid properties derived from this curve fit were $\sigma = 76 \pm 5$ mN/m and $\eta = 1.1 \pm 0.2$ mPa s, which are to be compared with the standard values for water at 20 °C of 72.8 mN/m and 1.0 mPa s. [20]

At early times the amplitude variation was greater than the limit of validity of the linear model (approximately ±10%) and also included significant contributions from modes higher than $l = 2$: no attempt was therefore made to fit these earlier shapes (as shown for example in Fig. 1). Table 2 shows the values of viscosity and surface tension obtained for pure water from two different drop sizes, giving different frequencies of oscillation. As expected for a Newtonian liquid, the viscosity showed no significant variation with frequency, and essentially the same value of surface tension was derived for both drop sizes.

Fig. 4 shows the amplitude variation for a 44 μm diameter drop of 1.1 wt% PEDOT:PSS solution, generated from images captured at 5×10^5 fps. The initial rapid change of shape (broken line) occurs during the collapse of the ligament into the main drop, and is followed by decaying oscillation about a spherical drop shape at 29 kHz. The solid line represents the predicted behaviour for a drop with surface tension of 44 ± 4 mN/m and a viscosity η' of 3.5 ± 0.7 mPa s.

Table 2
Properties of pure water derived by the oscillating drop method. Standard values for the surface tension and viscosity at 20 °C are 72.8 mN/m and 1.00 mPa s respectively [20].

Sample	Drop diameter (μm)	Oscillation frequency (kHz)	Surface tension σ (mN/m)	Viscosity η' (mPa s)
Water	31±1	62.7±0.2	76.5±7	1.1±0.2
	55±1	27.5±0.2	76.0±7	1.2±0.2
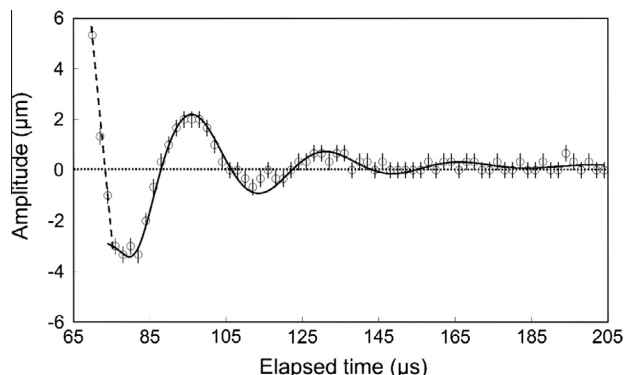
Fig. 4. Shape oscillation of a 1.1 wt% PEDOT:PSS droplet, with a diameter of 44 ± 1 μm. The initial rapid change (broken line) is not included in the curve fit which corresponds to a surface tension of 44 ± 4 mN/m and a viscosity of 3.5 ± 0.7 mPa s.

Fig. 5 shows data for a larger, 58 μm diameter drop of the same fluid oscillating at the lower frequency of 23 kHz. The effective surface tension σ was 60 ± 6 mN/m with a viscosity of 10±2 mPa s.

Table 3 summarises the results obtained for the 1.1 wt% aqueous PEDOT:PSS solutions with and without surfactants, while Table 4 gives results for 0.8 wt% aqueous PEDOT:PSS either with 30 wt% IPA or 0.06 wt% Dynol 607 surfactant. Values of surface tension and viscosity from conventional methods are listed for comparison. The results clearly show that at the high frequencies involved in drop oscillation, aqueous PEDOT:PSS exhibited quite different properties from those measured by more conventional methods at low frequencies and long timescales. The effective viscosity was much lower than the low shear rate values and the effective surface tension was significantly above the equilibrium (long timescale) value. However, the addition of Dynol 607 to excess (above its solubility limit) effectively lowered the surface tension to the equilibrium value.
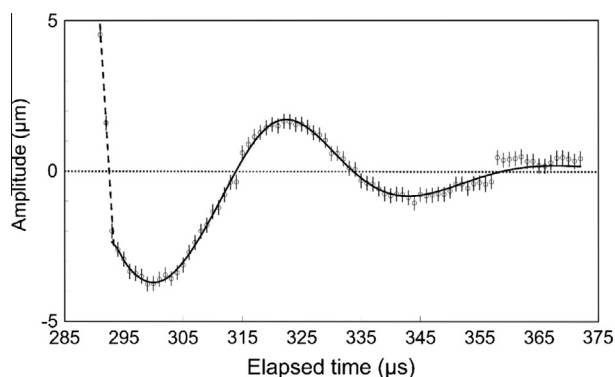

Fig. 3. Shape oscillations of a 31 ± 1 μm (40 pixel) diameter drop of pure water in terms of the amplitude $r_0 a_2(t) = (L - W)/3$. The uncertainty in amplitude due to measurement errors was estimated at ±0.26 μm. The solid line represents the behaviour predicted for a liquid with the density of water, viscosity of 1.1 mPa s and surface tension of 76.5 mN/m for the fundamental ($l = 2$) mode. The data points at early times which lie above and below the fitted curve correspond to higher-order, rapidly decaying modes.

Fig. 5. Oscillation of a 58 μm diameter 1.1 wt% PEDOT:PSS drop at 23 kHz. Ligament recoil drives the initial oscillation. A curve fit is shown for effective surface tension of 60 ± 6 mN/m and apparent viscosity 10 ± 2 mPa s.

Table 3
Properties derived from the oscillating drop (OD) method for 1.1 wt% PEDOT:PSS with Dynol 607 (D) and Zonyl FSO-100 (Z) surfactants, and for comparison, the values of surface tension and viscosity measured by conventional methods (CM) or by estimation (¶).

| D & Z (wt%)	Drop diameter (µm)	Oscillation frequency (kHz) (all ± 1 kHz)	Surface tension (OD) (mN/m)	Surface tension (CM) (mN/m)	Viscosity (OD) (mPa s)	Viscosity (CM) (mPa s)
None	53 ± 1	30	80 ± 8	70 ± 3	3.2 ± 0.6	63
0.23 D & 0.27 Z	44 ± 1	29	44 ± 4	21 ± 1	3.5 ± 0.7	68
ditto	46 ± 1	28	48 ± 5	21 ± 1	3.0 ± 0.6	68
ditto	44 ± 1	33	55 ± 6	21 ± 1	3.0 ± 0.6	68
ditto	57 ± 1	18	40 ± 4	21 ± 1	5 ± 1	68
ditto	58 ± 1	23	60 ± 6	21 ± 1	10 ± 2	68
0.33 D	52 ± 1	18	29 ± 3	30¶	3.0 ± 0.6	68
0.66 D	44 ± 1	24	33 ± 3	30¶	3.0 ± 0.6	68
ditto	55 ± 1	13	18 ± 2	30¶	2.2 ± 0.4	68

Table 4
Properties derived from OD and CM methods for 0.8 wt% PEDOT:PSS with 0.06 wt% Dynol 607 or 30 wt% isopropyl alcohol (IPA) additives.

Additive (wt%)	Drop diameter (µm)	Oscillation frequency (kHz)	Surface tension (OD) (mN/m)	Surface tension (CM) (mN/m)	Viscosity (OD) (mPa s)	Viscosity (CM) (mPa s)
30, IPA	53 ± 1	23	47 ± 5	30 ± 1	7.8 ± 1.5	25
	58 ± 1	20	45 ± 5	30 ± 1	3.6 ± 0.7	25
0.06, Dynol 607	52 ± 1	28	68 ± 7	30 ± 1	3.6 ± 0.7	25
ditto	49 ± 1	29	64 ± 6	30 ± 1	3.9 ± 0.8	25
ditto	50 ± 1	28	62 ± 6	30 ± 1	3.7 ± 0.8	25
ditto	50 ± 1	29	65 ± 6	30 ± 1	3.3 ± 0.7	25
ditto	53 ± 1	27	67 ± 7	30 ± 1	3.7 ± 0.8	25
ditto	51 ± 1	29	72 ± 7	30 ± 1	3.6 ± 0.7	25

While periodic damped oscillation of the drop shape was observed in nearly all experiments with PEDOT:PSS, in one case the drop failed to oscillate but instead exhibited a slow aperiodic decay towards its final spherical shape. A sequence of images is shown in Fig. 6 and the data extracted from this experiment is shown in Fig. 7(a), where it is compared with the more usual behaviour of an oscillating drop in Fig. 7(b). Both sets of data relate to the same liquid (containing 1.1 wt% PEDOT:PSS and 0.33 wt% Dynol 607); the data plotted in Fig. 7(b) relates to the images shown in Fig. 1. The two drops were of similar diameter (48 µm for the drop shown in Fig. 6 and 52 µm for that in Fig. 1), but while the derived values of surface tension in the two cases were also similar, those for viscosity were significantly different: 75 mPa s for the overdamped drop, and 3 mPa s for the oscillating drop.
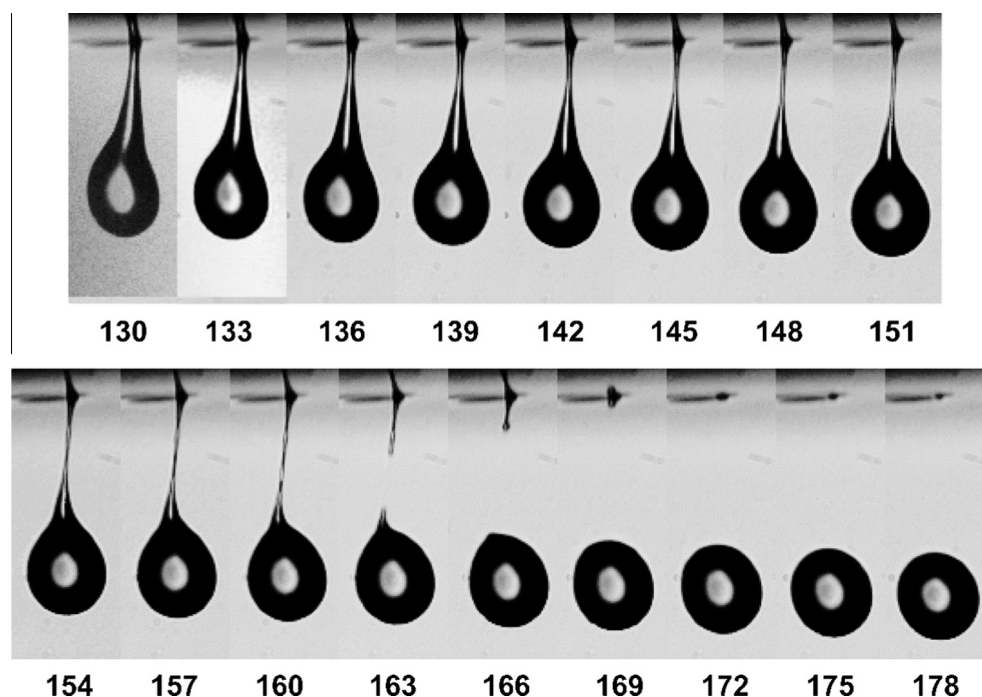
Fig. 6. Drop formation followed by aperiodic shape decay in 1.1 wt% PEDOT:PSS + 0.33 wt% Dynol 607. The elapsed time (µs) following emergence of the jet from the nozzle exit (visible at the top of each image) is shown below each image.
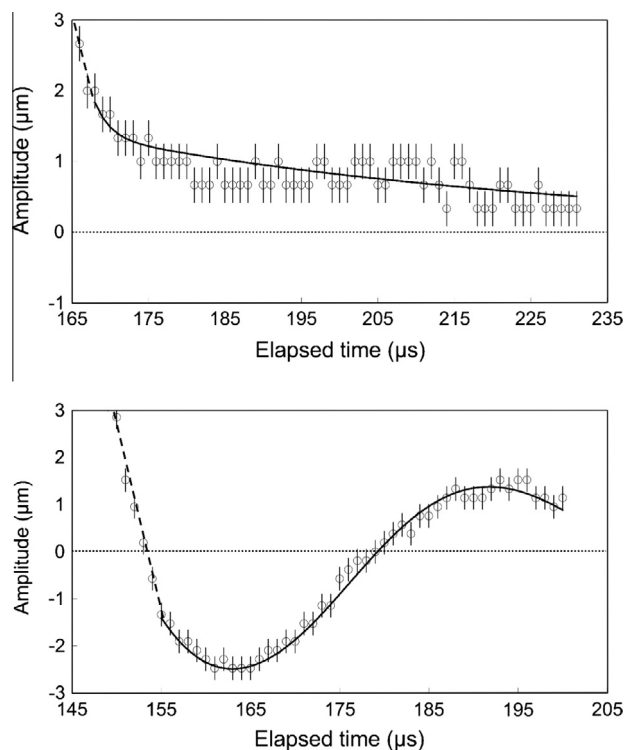
Fig. 7. Comparison of the behaviour of two drops of 1.1 wt% PEDOT:PSS with 0.33 wt% Dynol 607: (a) 48 μm diameter drop exhibiting a slow aperiodic shape decay consistent with surface tension of 26 mN/m and viscosity of 75 mPa s; (b) 52 μm diameter drop oscillating at 18 kHz with apparent surface tension 29 mN/m and viscosity 3 mPa s.

5. Discussion

The oscillating drop method has been widely used in previous work to estimate both surface tension and viscosity for Newtonian liquids, but in most cases with larger drops than those studied here which are representative of drop-on-demand inkjet printing. Yang et al. [8] showed the method to be reliable for drops of water and aqueous hydroxymethylcellulose solution ca. 60 μm in diameter, and the present results for pure water confirm that finding. Morita et al. [10] have applied it successfully to drops as small as 18 μm diameter, generated from a drop-on-demand printhead. However, for measuring fluid properties over a wide range of timescales the method does have some limitations. As is evident from Eq. (2) and the results in Table 2, for any given fluid (with particular values of surface tension and density) the frequency of drop oscillation is controlled by the drop size, and thus it is not possible to explore a wide range of frequencies by this method without using drops with a correspondingly wide range of sizes. Drop-on-demand inkjet printing involves drops from about 15 to 50 μm in diameter, and the range of oscillation frequencies which can be explored with drops generated by that method (but, also, which is relevant to DoD printing) is therefore small.

A further limitation is imposed by the requirement that the drop shape does change in a periodic manner, rather than exhibiting an aperiodic decay. This limits the viscosity of the liquid to which the method can be applied. For example, as discussed in Section 2, for a 50 μm diameter drop with the density of water and a surface tension of 32 mN/m the maximum viscosity at which the drop can be made to oscillate is 16 mPa s.

As shown in Fig. 2 and also demonstrated in earlier work [4], aqueous PEDOT:PSS exhibits marked shear-thinning behaviour in shear rheometry. The viscous and elastic components both fall with increasing frequency. Viscoelastic drop oscillation theory [6,12] can be used to estimate the time- and volume-averaged shear rates to be of the order of $2.5 \times 10^3 \text{ s}^{-1}$ for the 50 μm diameter drops generated here by drop-on-demand jetting. The high-shear rate limit to the fluid viscosity should therefore be approached and maintained within an oscillating drop, at least until the shear-rate falls so that the fluid can recover its viscosity.

For almost all the drops of aqueous PEDOT:PSS investigated in the present work, the viscosity values deduced from the decay of the shape oscillation and listed in Tables 3 and 4 were much smaller than the values measured by conventional methods at low shear rates: typically by a factor of up to 20. These values derived from the oscillating drop method (3–4 mPa s in most cases) can be compared with the values deduced from the work of Hoath et al. [4] They showed that the jet speeds attained by 1.1 wt% PEDOT:PSS solution in drop-on-demand inkjet printing were very similar to those achieved, under identical driving conditions, by a Newtonian water–glycerol mixture with a viscosity of 10 mPa s, suggesting that the viscosity of the PEDOT:PSS solution in the printhead nozzle must have been of a similar value, and thus much lower than the low-shear rate viscosity. However, although shear-thinning evidently occurs under the high shear-rate conditions to which the fluid is exposed in the printhead nozzle, two pieces of evidence suggest that the viscosity of the fluid then recovers rapidly. One is the observation reported by Hoath et al. [4] that the speed of radial thinning of the ligament behind the main drop, after it has left the nozzle, is consistent with a much higher value of viscosity.

The second is the observation, as illustrated by Figs. 6 and 7(a), that in certain circumstances the drop can exhibit the slow aperiodic shape decay characteristic of high viscosity rather than the periodic oscillation associated with a low viscosity (as shown in Fig. 7(b). The difference between these two types of behaviour is very marked, and the corresponding values of viscosity differ by a factor of about 20. The ages of the drops were similar (about 150–200 μs), but the magnitudes of the impulse delivered to these two drops by the collapse of the residual ligament were quite different, as shown by the sets of images in Figs. 1 and 6. This analysis suggests that collapse of a large ligament (as shown in Fig. 1) causes a large enough deformation of the drop that the associated deformation rate is sufficient to induce shear-thinning. The shear-thinned droplet then oscillates (for 50–100 μs) and the associated shear rate maintains the low viscosity states for as long as the drop continues to oscillate. An oscillation amplitude of 5% (i.e. 10% peak to peak) at 25 kHz would generate a shear rate of about 5000 s^{-1}, whereas 1% amplitude would correspond to shear rate of about 1000 s^{-1}, so the suggestion is not unreasonable. The less massive ligament of Fig. 6, in contrast, provides insufficiently high shear-rate conditions to cause significant shear-thinning in the drop surface, and subsequent shape changes in this more viscous drop remain over-damped.

These observations suggest that recovery of the viscosity to its low-shear value after ejection of the fluid from the nozzle, for these fluids, must be occurring on a timescale significantly shorter than 100 μs. Quantitative estimates of the effect of ligament retraction can be made from measurements of the images in Figs. 1 and 6. The retracting ligament shown in Fig. 1 has an initial volume about 17% of the final spherical drop volume, and its end moves at an initial speed relative to the main drop of 4.6 m/s. The ligament in Fig. 6, in contrast, represents only 1.8% of the total drop volume, and its initial tail speed was 5.1 m/s. The kinetic energy and momentum delivered to the two drops by ligament retraction thus differed by a factor of about 8.

Extrapolation of the measured viscosity values for 1.1 wt% PEDOT:PSS with surfactant shown in Fig. 2 suggests that at 30 kHz the viscosity should be 4.2 ± 0.1 mPa s, irrespective of

whether a power-law or Carreau model is used. The values derived from the oscillating drop experiments at similar frequencies (shown in Table 3) are somewhat lower at about 3.2 ± 0.6 mPa s. It is useful to examine whether this discrepancy might be accounted for by elastic properties of the fluid which are ignored in the simple analysis, by using the model of Khismatullin and Nadim [12]. Fig. 8 shows the non-dimensionalised decay factor and the non-dimensionalised frequency derived from both the asymptotic and full theories for a 53 μm diameter drop, assumed to have the density of water and a surface tension of 29 mN/m. The decay factor and frequency have been non-dimensionalised by division by the fundamental mode frequency Ω_2. If the difference between the oscillating drop measurements and the viscosity deduced from conventional rheometry, by a factor of 3.2/4.2 = 0.70, is indeed due to elasticity, then the equivalent non-dimensionalised decay factor, assuming the computed rate at $De_1 = 0$ in Fig. 8, is $0.70 \times 0.095 = 0.067$. Fig. 8 then implies the corresponding value of De_1 is 1.2 ± 0.6. This would correspond to a relaxation time λ_1 of 6 ± 3 μs, which is somewhat shorter than the timescales involved in the development and deformation of the oscillating drops (e.g. about 75 μs and 33 μs for the drop in Fig. 4), although viscoelastic timescales are comparable to Ω_2^{-1}, the inverse of the Lamb frequency. However, it is also possible that the difference in the viscosity values might be accounted for purely by experimental measurement errors, which can be estimated at ±20%.

The values of surface tension derived from the oscillating drop method for pure water (shown in Table 2) and for the 1.1% PEDOT:PSS solution without surfactant were, within experimental error, the same as those measured by the conventional method of bubble tensiometry. It should be noted that the accuracy of the derived value of surface tension is very sensitive to any error in the measurement of drop diameter, with a 3% error in the latter corresponding to almost 10% error in surface tension. However, very significant differences between the values of surface tension measured in the two different ways were found for the PEDOT:PSS solutions with added surfactant.

For both concentrations of PEDOT:PSS, addition of the anionic organic surfactant Dynol 607 at all the concentrations investigated led to a marked reduction in the conventionally-measured surface tension, from ca. 80 mN/m without the surfactant to ca. 30 mN/m with. Further addition of Zonyl FSO-100, a non-ionic fluorosurfactant, led to a further reduction to ca. 21 mN/m. However, the values of surface tension derived from the oscillating drop

measurements were much higher, with mean values ranging from 66 mN for 0.06 wt% Dynol to 27 mN for 0.66 wt% Dynol, and 46 mN/m for the solutions containing 0.23 wt% Dynol and 0.27 wt% Zonyl. These values are consistent with the time-dependence of surface tension expected under the conditions of the oscillating drop experiment, in which the typical surface age of the drop was 100–300 μs, much smaller than the diffusion time for the surfactant which can be estimated [8] to be about 4 ms. Dynamic surface tension effects are also clear in the water–isopropanol mixture, which exhibited a surface tension of 30 mN/m in bubble tensiometry but a higher value of 46 mN/m in the oscillating drop experiments. The oscillating drop thus provides a sensitive method to probe surface tension at a timescale which is relevant to jet and drop formation in inkjet printing, which is inaccessible to more conventional methods of measurement.

6. Conclusions

The oscillating drop method provides a sensitive and accurate method for determining surface tension and viscosity of complex fluids under the conditions relevant to drop-on-demand inkjet printing. Surface tension at the surface age of the drop in flight can be derived from measurement of the drop oscillation frequency. For the surfactant-containing aqueous solutions investigated here, and also for a water–isopropanol mixture, the surface tensions were significantly higher than those measured by more conventional methods, because the surface ages of the drops were less than the surfactant migration times.

The viscosity of the fluid can be derived from measurement of the decay of the drop oscillation, and for the aqueous PEDOT:PSS investigated here marked shear-thinning was detected from the oscillating drop measurements. Shear-thinning was also observed in conventional rheometry, although the values of viscosity derived from the oscillating drop experiments were slightly lower than those deduced from high shear-rate rheometry. Viscoelastic effects are small (and quite possibly negligible) but may contribute to this difference: a relaxation time of <10 μs was deduced, somewhat shorter than the other timescales involved in (inkjet) drop production or oscillation.

In drop-on-demand inkjet printing the fluid is subjected to a very high shear rate (typically 10^5 s^{-1}) within the nozzle, which in a susceptible fluid causes shear-thinning during jetting. However, the oscillating drop is observed after drop ejection (typically 300 μs later) and this work provides strong evidence that within that timescale, for aqueous PEDOT:PSS, the viscosity recovers to its low-shear value. If the drop is then subjected to only slight perturbation, for example through the retraction of a very slender ligament, the viscosity remains high. In most cases, however, the retraction of the ligament provides a larger stimulus which causes sufficient deformation to provide effective shear-thinning in the oscillating drop. It is evident that in modelling jet and drop formation for non-Newtonian fluids, an accurate constitutive equation is needed which takes account of history as well as current deformation rate.
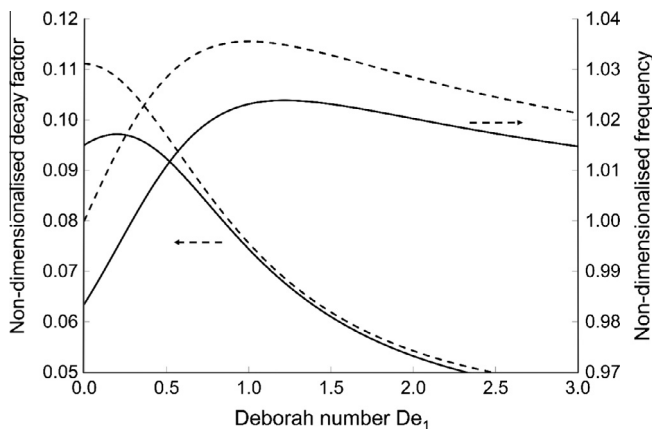
Fig. 8. Values of decay factor and oscillation frequency computed from the asymptotic (dashed lines) and full (solid lines) viscoelastic theory [12] for an aqueous 1.1 wt% PEDOT:PSS drop with $Re = 45$ and $De_2/De_1 = 0.36$. These values have been non-dimensionalised by dividing by the fundamental mode frequency Ω_2.

References

[1] O.A. Basaran, H.J. Gao, P.P. Bhat, Non-standard inkjets, Ann. Rev. Fluid Mech. 45 (2013) 85–113.

[2] H. Sirringhaus, T. Kawase, R.H. Friend, T. Shimoda, M. Inbasekaran, W. Wu, E.P. Woo, High-resolution inkjet printing of all-polymer transistor circuits, Science 290 (2000) 2123–2126.

[3] S.J. Jung, A. Sou, E. Gili, H. Sirringhaus, Inkjet-printed resistors with a wide resistance range for printed read-only memory applications, Org. Electron. 14 (2013) 699–702.

[4] S.D. Hoath, S. Jung, W.K. Hsiao, I.M. Hutchings, How PEDOT:PSS solutions produce satellite-free inkjets, Org. Electron. 13 (2012) 3259–3262.

[5] S.D. Hoath, W.K. Hsiao, S. Jung, G.D. Martin, I.M. Hutchings, N.F. Morrison, O.G. Harlen, Drop speeds from drop-on-demand inkjet print-heads, J. Imag. Sci. Technol. 57 (2013) 010503.

[6] G. Brenn, S. Teichtmeister, Linear shape oscillations and polymeric timescales of viscoelastic drops, J. Fluid Mech. 733 (2013) 504–527.

[7] S.D. Hoath, S. Jung, I.M. Hutchings, Simple criterion for jet break up in drop-on-demand inkjet printing, Phys. Fluids 25 (2013) 021701.

[8] L.S. Yang, B.K. Kazmierski, S.D. Hoath, S. Jung, W.-K. Hsiao, Yiwei Wang, A. Berson, O.G. Harlen, N. Kapur, C.D. Bain, Determination of dynamic surface tension and viscosity of non-Newtonian fluids from drop oscillations, Phys. Fluids 26 (2014) 113103.

[9] T. Ishiwata, K. Sakai, Dynamic surface tension measurement with temporal resolution on microsecond scale, Appl. Phys. Exp. 7 (2014) 077301, http://dx.doi.org/10.7567/APEX.7.077301.

[10] N. Morita, S. Hirakata, T. Hamazaki, Study on vibration behavior of jetted ink droplets and nozzle clogging, J. Imag. Soc. Jpn. 49 (2010) 14–19. http://dx.doi.org/10.11370/isj.49.14.

[11] H. Lamb, Hydrodynamics, sixth ed., Cambridge University Press, 1932. pp. 473–475.

[12] D.B. Khismatullin, A. Nadim, Shape oscillations of a viscoelastic drop, Phys. Rev. E 63 (2001) 061508.

[13] P.J. Carreau, D. Dekee, M. Daroux, An analysis of the viscous behavior of polymeric solutions, Can. J. Chem. Eng. 57 (1979) 135–140.

[14] H. Giesekus, A unified approach to a variety of constitutive models for polymer fluids based on the concept of configuration-dependent molecular mobility, Rheol. Acta 21 (1982) 366–375.

[15] H. Giesekus, Constitutive-equations for polymer fluids based on the concept of configuration-dependent molecular mobility – a generalized mean-configuration model, J. Non-Newt. Fluid Mech. 17 (1985) 349–372.

[16] J.W.S. Rayleigh, Proc. Roy. Soc. 29 (1879) 71–97 (Appendix II therein).

[17] A. Prosperetti, Free oscillations of drops and bubbles – the initial-value problem, J. Fluid Mech. 100 (1980) 333–347.

[18] E. Becker, W.J. Hiller, T.A. Kowalewski, Experimental and theoretical investigation of large-amplitude oscillations of liquid droplets, J. Fluid Mech. 231 (1991) 189–210.

[19] W.R. Smith, Modulation equations for strongly nonlinear oscillations of an incompressible viscous drop, J. Fluid Mech. 654 (2010) 141–159. http://dx.doi.org/10.1017/S0022112010000480.

[20] Kaye and Laby. www.kayelaby.npl.co.uk.

[21] D.C. Vadillo, T.R. Tuladhar, A. Mulji, M.R. Mackley, The rheological characterisation of linear viscoelasticity for ink jet fluids using piezo axial vibrator (PAV) and torsion resonator (TR) rheometers, J. Rheol. 54 (2010) 781–795.